Cation localization and movement within DNA thrombin binding aptamer in solution†

Marko Trajkovski,[a] Primož Šket[a] and Janez Plavec*[a,b]

Received 21st July 2009, Accepted 18th August 2009
First published as an Advance Article on the web 21st September 2009
DOI: 10.1039/b914783g

The thrombin binding aptamer, 15-mer oligonucleotide d[$G_2T_2G_2TGTG_2T_2G_2$], was folded into the well known antiparallel unimolecular G-quadruplex in the presence of $^{15}NH_4^+$ ions. Although the formed G-quadruplex is thermodynamically less stable than in the presence of K^+ ions, the loop conformations and folding topology are the same. On the other hand, titration of Na^+ ions into an aqueous solution of TBA resulted in the formation of one major and several minor species of G-quadruplexes. Solution-state NMR was used to localize $^{15}NH_4^+$ ions between the two G-quartets within the core of the structure, and to determine the equilibrium binding constant, which equals 190 M^{-1}. No other potential cation binding sites were resolved on the time-scale of NMR spectrometer. Exchange of $^{15}NH_4^+$ ions between the inner binding site and bulk solution is characterized by the exchange rate constant of 1.0 s^{-1} at 15 °C. T4 and T13 form a noncanonical base pair, which greatly affects access of bulk ions into the cation binding site in the G-quadruplex core. G2 and G11 exhibit out of plane bending towards the two TT loops away from the bound $^{15}NH_4^+$ ions, which in turn exposes them to more efficient chemical exchange processes with bulk ions and water.

Introduction

The importance of biological roles of G-quadruplexes, four-stranded structural elements that appear in both DNA and RNA, has been accumulating through the identification of a large number of potentially quadruplex-forming repeats in telomere sequences and in promoter regions of genes, promising pharmaceutical activity and discovery of proteins that specifically recognize quadruplexes as well as applicability in nanotechnology. It has been known for several years that not only the primary nucleotide sequence, but also environmental conditions, and in particular cations, play an important role in the formation, topology and stability of G-quadruplexes. Nucleic acid aptamers attract considerable interest due to their high specificity towards biologically important molecules that makes them interesting therapeutic agents. In 1992 oligonucleotide d[$G_2T_2G_2TGTG_2T_2G_2$] (below noted as TBA, for thrombin binding aptamer) was identified as a potential anticoagulant with a high binding affinity to thrombin.[1] Later efforts led to the characterization of TBA under various conditions with the objective of exploring its potential for medical application. Modulation of the original TBA sequence resulted in changed biophysical properties and anticoagulant activity that were in some, but not in all, cases attributed to different folding topologies and different molecularities.[2–8] The first 3D structure of the TBA quadruplex was determined by NMR in the presence of K^+ ions.[9–12] TBA was shown to form a unimolecular antiparallel G-quadruplex with two G-quartets and three lateral loops, a central TGT loop and two TT loops (Fig. 1). The solution state NMR structure was consistent with the X-ray diffraction data.[13] Later studies focused on folding and stability in the presence of various metal ions including divalent Sr^{2+}, Pb^{2+} and Mn^{2+} ions.[14–20] Many co-solvents and small molecular solutes increase the thermal stability of TBA G-quadruplex.[21,22]

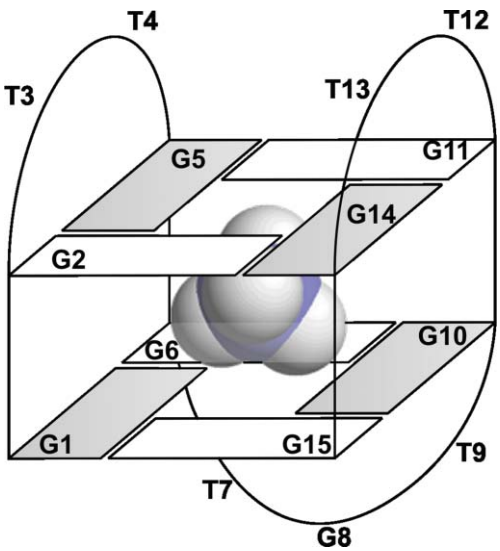

Fig. 1 Schematic presentation of a chair-type G-quadruplex topology of TBA, d[$G_2T_2G_2TGTG_2T_2G_2$], with an ammonium ion located between the G-quartets. White and gray squares represent guanine bases in *anti* and *syn* conformations, respectively. For clarity, the bases of the loop residues are not shown.

The unimolecular TBA quadruplex with a chair type topology represents an interesting model system that enables investigation of cation binding and thus the role of cations on stability and

[a]*Slovenian NMR Centre, National Institute of Chemistry, Hajdrihova 19, SI-1000, Ljubljana, Slovenia. E-mail: janez.plavec@ki.si; Fax: +386 (0)147 60 300; Tel: +386 (0)147 60 353*
[b]*Faculty of Chemistry and Chemical Technology, University of Ljubljana, SI-1000, Ljubljana, Slovenia*

† Electronic supplementary information (ESI) available: ROESY NMR spectra. See DOI: 10.1039/b914783g

structure of a G-quadruplex. In parallel with the general trends of G-quadruplex stabilization, K^+ ions were shown to stabilize the TBA quadruplex better than Na^+ ions.[14,23] NMR studies by Bolton *et al.* suggested that there are two K^+ ion binding sites that are occupied in a sequential manner as the cation concentration increases, and that their binding is associated with structural changes.[24] Later studies by the groups of Shafer[17,18] and Marky[14,15] showed that Pb^{2+} and Sr^{2+} ions form M^{2+}–TBA complexes in 1 : 1 stoichiometry. Furthermore, both groups showed that Pb^{2+} and Sr^{2+} ions occupy the central cavity of the G-quadruplex structures between the two G-quartet planes. Interestingly, the ionic radii of Sr^{2+} and Pb^{2+} are slightly smaller than that of a K^+ ion. On the other hand, the charge density of the two divalent cations is larger. Another interesting difference was noted in the inter-quartet distance, which was *ca.* 0.7 Å larger in the case of Sr^{2+} in comparison to K^+ ions.[15]

Ammonium ions have been shown to stabilize the TBA quadruplex to an extent that is similar to that observed for K^+ albeit with a *ca.* 20 °C lower T_m value.[14] Isotopically ^{15}N-labeled ammonium ions in combination with ^1H–^1H and ^{15}N–^1H NMR correlation experiments have proved themselves a superb solution-state probe of monovalent cation coordination sites.[25–32] Furthermore, $^{15}NH_4^+$ ions have been used extensively to evaluate the dynamics of cations coordinated within G-quadruplexes. NMR studies utilizing $^{15}NH_4^+$ ions as a probe for localizing cation binding sites and for monitoring the movement of cations between different coordination sites reveal that $^{15}NH_4^+$ ions move along the central axis of the G-quadruplexes and solution in a manner that is reminiscent of an ion channel. Our recent analysis of $^{15}NH_4^+$ ion movement within d[$(G_3T_4G_4)_2$], a bimolecular G-quadruplex, demonstrates the absence of $^{15}NH_4^+$ ion movement between the two binding sites along the central ion cavity of the G-quadruplex structure.[29] However, $^{15}NH_4^+$ ions were shown to move between the two binding sites, U and L, and bulk solution. $^{15}NH_4^+$ ion movements from the binding sites U and L into the bulk solution have been characterized by residence lifetimes of 139 ms and 1.7 s at 25 °C, respectively. The 12-times faster movement from binding site U has demonstrated that $^{15}NH_4^+$ ion movement is controlled by the structure of T_4-loop residues which, through diagonal—*versus* lateral—type orientations, imposes distinct steric restraints for cations to leave or enter the G-quadruplex core.[29] In a related study, $^{15}NH_4^+$ ion movement between the interior of the unimolecular d[$G_4(T_4G_4)_3$] G-quadruplex and bulk solution was demonstrated to be five-times faster from the outer binding site (named O2) spanned by the two lateral loops in comparison to that from the O1 binding site spanned by a diagonal loop.[30] In the above studies, the difference in the rates of $^{15}NH_4^+$ ion movements from the two (outer) binding sites was associated with the loop topologies that span their outer G-quartets.

In the current study the ability of $^{15}NH_4^+$ ions to induce TBA to fold into a G-quadruplex in comparison to K^+ and Na^+ ions, and their specific cation localization within the TBA G-quadruplex was evaluated with the use of heteronuclear NMR and other spectroscopic methods. Our initial observations did not support earlier reports[24] that one of the K^+ ion binding sites was supposedly between the T7–G8–T9 loop and the neighbouring G-quartet, and the other one between the T3–T4 and T12–T13 loops and the G-quartet. One of the most important findings of the current study is that monovalent cations are indeed localized between the two G-quartets in the core of unimolecular TBA quadruplex, and not between the G-quartets and the lateral loops as has been suggested earlier.[23,24] Furthermore, we did not observe resolved signals for $^{15}NH_4^+$ ions that would correspond to the 'expected' binding sites. In addition, the study of binding and movement of ammonium ions in a chair type topology offers new insights on the role of lateral-type loops in controlling the passage of cations thought the central ion channel that has not been studied before. NMR spectra that experimentally verify both localization and cation movement are rather unique in the studies of DNA. In this way, G-quadruplexes represent a unique system that allows study of kinetics of cation movement in aqueous solution. The acquired new data will help to better understand the role of cation interactions for aptamer structure adopted by the 15-mer oligonucleotide with therapeutic importance for blocking blood clot formation.

Results

Folding of TBA in the presence of $^{15}NH_4^+$, K^+ and Na^+ ions

The formation of the TBA G-quadruplex was initially followed by monitoring proton resonances as a function of increasing $^{15}NH_4^+$ ion concentration. Eight narrow and well resolved imino resonances were observed in the 1D ^1H NMR spectrum in the range from 11.65 to 12.29 ppm, which is consistent with the formation of a single G-quadruplex species containing two G-quartets (Fig. 2a). For comparison, TBA has also been folded into a G-quadruplex structure in the presence of K^+ ions. The 1D ^1H NMR spectrum presented in Fig. 2b is in agreement with the published data.[9,10,12,23,24] Titration of Na^+ ions into an aqueous solution of TBA resulted in the formation of one major and several minor species of G-quadruplexes (Fig. 2c). Imino proton signals of the major species in the presence of Na^+ ions are in the range from 12.05 to 12.42 ppm. Additional signals in the range from 11.10 to 11.90 ppm are consistent with the chemical shift range reported for parallel G-quadruplex adopted by a ribo analogue of TBA in the presence of K^+ ions.[3] The ratio of the major species to other forms including unstructured TBA was increased by lowering the temperature from 15 to 2 °C, albeit more structures were still present.

CD spectra for TBA in the presence of $^{15}NH_4^+$ and K^+ ions shown in Fig. 3 are consistent with the formation of an antiparallel G-quadruplex.[3,14,18,21,22,33–35] The CD spectrum acquired in the presence of Na^+ ions is similar to the spectra of TBA in the presence of $^{15}NH_4^+$ and K^+ ions although unfolded and/or a parallel G-quadruplex(es) are also present in the equilibrium mixture.

Using pulsed-field gradient spin-echo experiments we determined translational diffusion constants, D_t, of TBA G-quadruplexes in the presence of $^{15}NH_4^+$ ions ($D_t = 1.24 \pm 0.02 \times 10^{-6}$ cm^2 s^{-1}), K^+ ions ($D_t = 1.20 \pm 0.05 \times 10^{-6}$ cm^2 s^{-1}) and Na^+ ions ($D_t = 1.28 \pm 0.06 \times 10^{-6}$ cm^2 s^{-1}) at 15 °C. Major and minor species in the presence of Na^+ ions exhibited equivalent translational diffusion constants suggesting similar shape and size of G-quadruplexes. Relying on the spherical model and considering the hydration layer of 2.8 Å the calculated diameters for the TBA G-quadruplexes in the presence of $^{15}NH_4^+$, K^+ and Na^+ ions were 24, 25 and 23 Å, respectively, with the error limits of ±1 Å.[36] All three diameters were in good agreement with the values

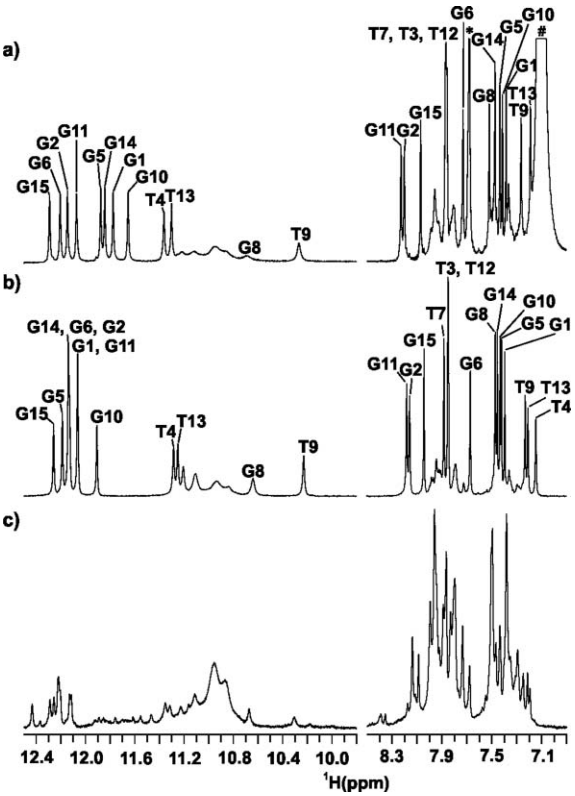

Fig. 2 Imino and aromatic regions of the ^{1}H NMR spectra of TBA at 15 °C in 5% $^{2}H_2O$, pH 6.0 and oligonucleotide concentration of 2.6 mM in the presence of (a) 52 mM $^{15}NH_4Cl$, (b) 10 mM KCl and (c) 104 mM NaCl. In panel (a) ^{1}H signals of $^{15}NH_4^+$ ions bound within the TBA G-quadruplex and in bulk solution are marked with * and #, respectively. The spectrum in panel (c) was not assigned due to the presence of multiple species of TBA G-quadruplexes.

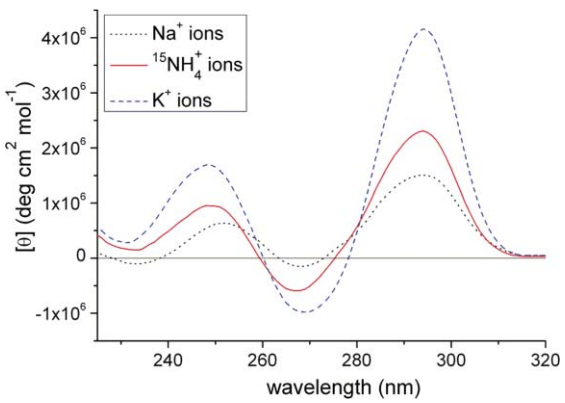

Fig. 3 CD spectra of TBA at 10.5 °C in the presence of NaCl (dotted line), KCl (dashed line) and $^{15}NH_4Cl$ (continuous line). The oligonucleotide concentration was 50 μM and salt concentration was 100 mM for all the three samples.

calculated with the HYDROPRO program[37] using coordinates from two known NMR structures (25 Å for PDB ID 148D and 26 Å for PDB ID 1RDE).[12,15]

The aromatic–anomeric region of 2D NOESY spectra of TBA in the presence of $^{15}NH_4^+$ ions reveals four guanine residues (G1, G5, G10 and G14) in *syn* and four guanine residues (G2, G6, G11 and G15) in *anti* conformation (Fig. 4). A sequential assignment

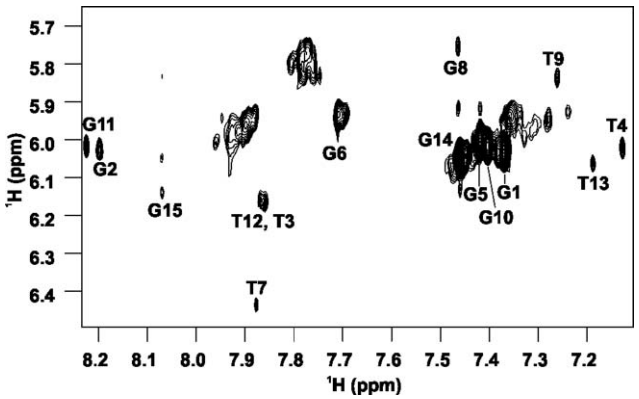

Fig. 4 Aromatic–anomeric region of NOESY spectrum of TBA with mixing time of 150 ms in the presence of 30 mM $^{15}NH_4Cl$ in 100% $^{2}H_2O$ at 15 °C. The oligonucleotide concentration was 1.5 mM.

revealed four 5′-*syn*-3′-*anti* steps with forward as well as backwards sequential H8–H1′ connectivities. Imino and aromatic protons were completely assigned with the use of NOESY and jump-and-return HMBC spectra. Interestingly, imino and H8 proton signals of guanines in *anti* conformation are deshielded with respect to guanines in *syn* conformation (Fig. 2a). Further examination of other regions of NOESY spectra confirmed formation of a G-quadruplex structure with the same general fold in the presence of $^{15}NH_4^+$ and K^+ ions. From ^{1}H and 2D NOESY spectra of the sample folded in the presence of Na^+ ions it was not possible to assign minor nor major species of TBA G-quadruplexes.

Loop conformations

Imino protons of T4 and T13 exhibited the narrowest signals of loop residues and furthermore were observed at pH values and temperatures where imino proton signals of other residues in the loops were broadened to the baseline. Methyl and H3 protons of T4 exhibited NOE contacts with imino protons of G2 and G5, respectively. Analogous NOE interactions were observed between T13-Me and T13-H3 with G11-H1 and G14-H1, respectively. Relative orientation of T4 and T13 are further substantiated by NOE interactions between T4-Me and G2-H8, and T13-Me and G11-H8. T3, T9 and T12 imino proton signals were observed at pH values lower than 6.0. The orientations of T3 and T12 residues were defined by sequential NOE interactions between their Me and H6 protons with T4 and T13 Me groups. The imino proton signal of T9 was narrower than the signals of T3 and T12 (Fig. 5). G8-H1 could be observed only in the narrow range around pH 6.0, whereas T7-H3 was not observed in the pH range from 4.5 to 7.0. The imino proton signals of residues in the loops became narrower by lowering the temperature from 15 to 2 °C. pH and temperature-dependent changes were reversible and were most pronounced for imino proton signals of T3, G8 and T12.

Given that TBA G-quadruplex adopted the same topology in the presence of $^{15}NH_4^+$ ions as with K^+ ions we further examined potential differences in the structure of the loops. Relative volumes of cross-peaks in NOESY spectra between methyl group protons of T9 and imino protons of G1, G6, G10 and G15 were the same in the presence of K^+ and $^{15}NH_4^+$ ions (Fig. 6). Distances between T9-Me and the imino protons of the outer G-quartet decrease in the following order: G15 > G1 > G10 > G6. Cross-peaks

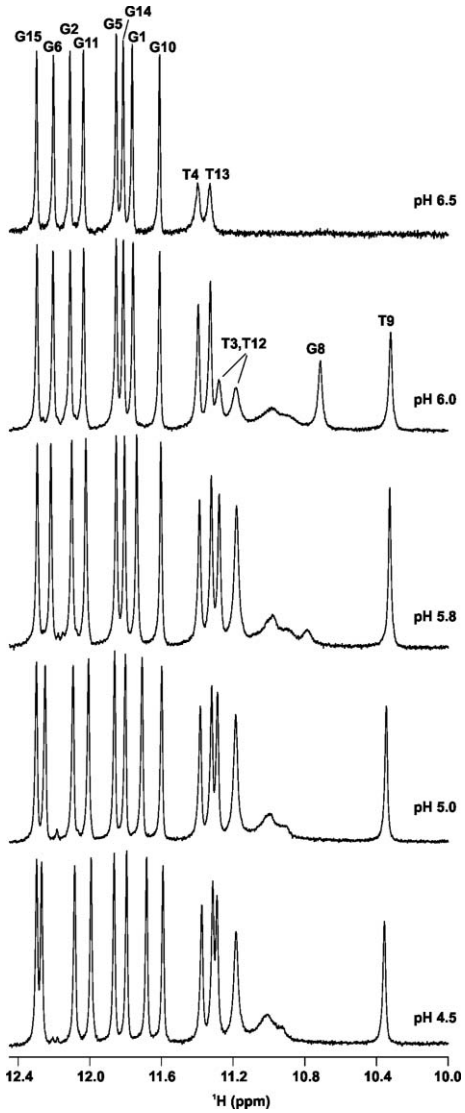

Fig. 5 Imino region of the ^{1}H NMR spectra of TBA at different pH values in the presence of 36 mM $^{15}NH_4Cl$ in 5% $^{2}H_2O$ at 5 °C. The oligonucleotide concentration was 1.8 mM.

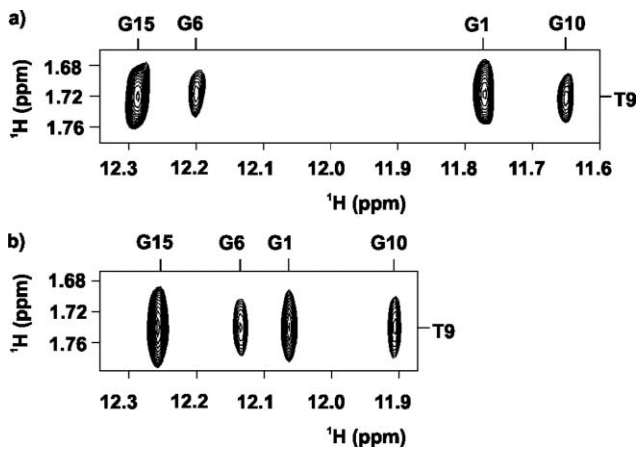

Fig. 6 Imino–methyl region of NOESY spectra of TBA with mixing time of 80 ms at 15 °C in the presence of (a) 36 mM $^{15}NH_4Cl$, pH 4.5 and (b) 3 mM KCl, pH 6.5. The oligonucleotide concentration was 1.8 mM.

between T9-H6 and T9-H1′ with G10 imino proton suggest that the two residues are stacked. The distances between T4 and G5 imino protons, and T13 and G14 imino protons at 15 °C in the presence of $^{15}NH_4^+$ and K^+ ions were different by less than 0.3 Å. In conclusion, the above comparisons and other NMR data on T4, T9 and T13 suggest that the two TT loops and the TGT loop adopt similar structures in the presence of $^{15}NH_4^+$ and K^+ ions.

$^{15}NH_4^+$ ions are localized between the two G-quartets

^{15}N–^{1}H filtered HSQC spectrum of TBA in the presence of $^{15}NH_4^+$ ions revealed two well resolved cross-peaks with ^{1}H chemical shifts of 7.10 and 7.68 ppm, which corresponded to $^{15}NH_4^+$ ions in bulk solution and bound within TBA G-quadruplex, respectively. ROESY spectrum was used to assign the signal at δ 7.68 ppm and thus localize bound $^{15}NH_4^+$ ions to the inner binding site (**I**) within G2→G14→G11→G5 and G1→G6→G10→G15 quartets (Fig. 7). Interestingly, volumes of cross-peaks between $^{15}NH_4^+$ ions at binding site **I** and imino protons of G2 and G11 were *ca.* 20% smaller than the volumes of cross-peaks with the other six guanines involved in the two G-quartets.

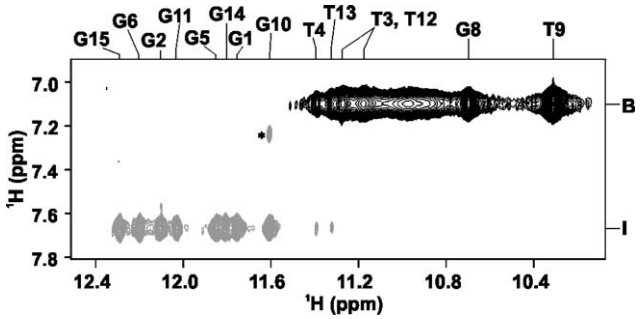

Fig. 7 ROESY spectrum of TBA with mixing time of 40 ms in the presence of 36 mM $^{15}NH_4Cl$ in 5% $^{2}H_2O$ at 5 °C and pH 6.0. The oligonucleotide concentration was 1.8 mM. Cross-peaks between $^{15}NH_4^+$ ions localized at the binding site **I** and the nearby imino protons are shown in gray, while exchange cross-peaks between $^{15}NH_4^+$ ions in bulk solution, **B**, and imino protons of residues in the loops are shown in black. * indicates a cross-peak between G10 imino proton and T9 H6.

Additional ROE cross-peaks were observed between $^{15}NH_4^+$ ions at binding site **I** and T4 and T13, but were approximately 10 times weaker than the corresponding cross-peaks to imino protons of guanines in the G-quartets (Fig. 7). No $^{15}NH_4^+$ ion localization was established in the proximity of the TGT loop. In order to observe a resolved signal with the chemical shift difference above 10 Hz from the bulk signal the corresponding residence lifetime τ ($\tau \times \Delta\delta \approx 1/2\pi$) would be below 16 ms. As such a signal was not observed on ^{1}H NMR time-scale the potential interactions of $^{15}NH_4^+$ ions near the three loops must be short-lived.

ROESY spectra, in addition, showed exchange cross-peaks between bulk $^{15}NH_4^+$ ions and imino protons of T3, T4, G8, T9, T12 and T13 (Fig. 7). The volumes of exchange cross-peaks between bulk $^{15}NH_4^+$ ions and imino protons of T3 and T12 were larger than with imino protons of T4 and T13. However, the largest exchange cross-peak was with T9 (Fig. 7).

Interestingly, ROE cross-peaks at the chemical shift of bulk water with the imino protons of guanines in G-quartets were observed. The volumes of the cross-peaks between bulk water and imino protons of G2 and G11 were larger than with the other six guanines in G-quartets in the presence of $^{15}NH_4^+$ ions (Figure S1†). A similar observation was made in the presence of K^+ ions (Figure S2†). Analysis of ROESY spectra in the presence of $^{15}NH_4^+$ and K^+ ions, in addition, revealed exchange cross-peaks of bulk water with imino protons of loop residues.

Determination of the binding constant of $^{15}NH_4^+$ ions to a TBA G-quadruplex based on the volume intensity of the cross-peak **I** in ^{15}N–^1H HSQC spectra as a function of concentration of added $^{15}NH_4^+$ ions afforded a value of 190 ± 30 M^{-1}.

$^{15}NH_4^+$ ion movement between the binding site I and bulk solution

Analysis of the ^{15}N–^1H NzExHSQC spectrum shown in Fig. 8 reveals two autocorrelation peaks corresponding to $^{15}NH_4^+$ ions localized at binding site **I** and in bulk solution (**B**). In addition to the autocorrelation peaks, we observed a cross-peak **IB** corresponding to the movement of $^{15}NH_4^+$ ions out of the interior of the G-quadruplex. The volume decrease of autocorrelation peaks **I** and **B**, and variation of volume of cross-peak **IB** in NzExHSQC spectra with mixing time has been described by biexponential functions (eqn (1) and (2)).[29] An iterative fit of parameters in eqn (2) to the experimental data provided an exchange rate constant (k_{IB}) of 1.0 ± 0.1 s^{-1} for $^{15}NH_4^+$ ion movement from binding site **I** to bulk solution (Fig. 9). The corresponding cross-peak **BI** was observed but could not be analyzed quantitatively due to its broad shape.

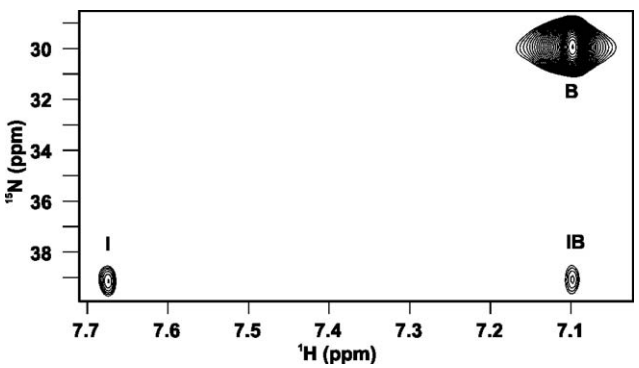

Fig. 8 2D ^{15}N–^1H NzExHSQC spectrum of TBA with mixing time of 1500 ms in the presence of 36 mM $^{15}NH_4Cl$ in 5% ^2H_2O at 15 °C and pH 4.5. The oligonucleotide concentration was 1.8 mM. Autocorrelation peaks for $^{15}NH_4^+$ ions at the binding site **I** and in bulk solution are labeled with **I** and **B**, respectively. A cross-peak indicating $^{15}NH_4^+$ ion movement from the binding site **I** to bulk solution is labeled with **IB**.

Cation dependent melting behaviour of the TBA G-quadruplex

UV spectroscopy was used to analyze melting transitions for TBA in solution in the presence of K^+ and NH_4^+ ions (Fig. 10). The melting and annealing processes in the presence of both cations were reversible. The temperatures at half transition for the TBA G-quadruplex in the presence of K^+ and NH_4^+ ions were 42.5 °C and 30.5 °C, respectively.

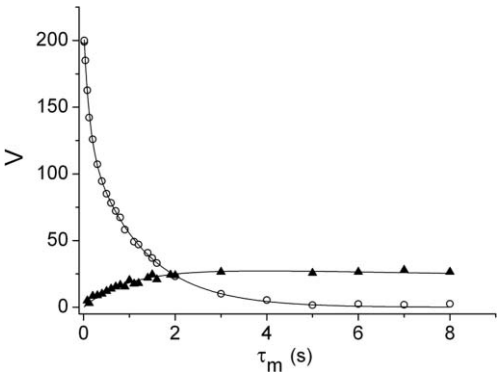

Fig. 9 Relative volumes of autocorrelation peak **I** (empty circles) and cross-peak **IB** (filled triangles) as a function of mixing time (τ_m) at 15 °C. Curves represent the best fits of the parameters in eqn (1) (A_1 = 129 ± 3, A_2 = 81 ± 3, B_1 = 8.4 ± 0.6 s^{-1} and B_2 = 0.84 ± 0.01 s^{-1}, individual deviations below 2.5 and rmsd = 0.8 arbitrary volume units, R = 0.999) and 2 (f = 0.145 ± 0.004, k_{IB} = 1.0 ± 0.1 s^{-1}, A and T_1 were held fixed at A = 210 and T_1 = 44 s, individual deviations below 7.2, rmsd = 5.4 arbitrary volume units, R = 0.990) to experimental data.

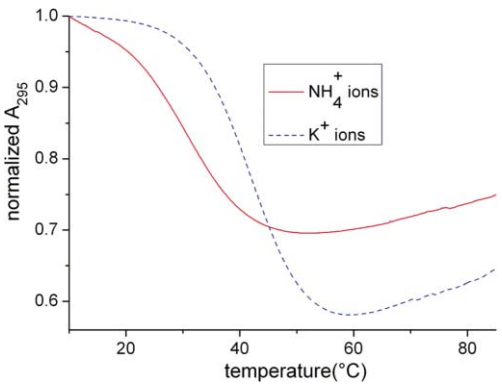

Fig. 10 UV melting profiles of TBA in the presence of NH_4^+ (continuous line) and K^+ (dashed line) ions. The concentrations of oligonucleotide were 24 μM and 34 μM, respectively. The corresponding cation concentrations were 50 mM and 10 mM.

Discussion

Our NMR data have shown that TBA in the presence of $^{15}NH_4^+$ ions forms a G-quadruplex with similar topology as in the presence of K^+, Sr^{2+} and Pb^{2+} ions.[9–13,15,17] Na^+ ions induce TBA G-quadruplex folding, but do not lead to a single structure even at relatively high cation concentrations. In ^1H NMR spectra of TBA in the presence of $^{15}NH_4^+$ ions, in addition to the eight imino protons of guanines involved in G-quartets, T4 and T13 exhibit sharp imino protons over a 4.5–6.5 pH range, which are indicative of a noncanonical base pair. T3, T9 and T12 imino proton signals were observed at pH values below 6.0. The G8 imino proton signal could be observed only in the narrow range around pH 6.0, whereas the T7 imino proton was not observed in the pH range from 4.5 to 7.0.

Translational diffusion constants obtained by pulse-field gradient NMR experiments in the presence of $^{15}NH_4^+$, K^+ and Na^+ ions afforded hydrodynamic radii between 23 and 25 Å which were consistent with an unimolecular G-quadruplex fold. Varra and co-workers have concluded recently, based on

concentration-dependent CD experiments, that acyclic analogues of TBA form a bimolecular G-quadruplex in the presence of potassium buffer (100 mM KCl, 10 mM K-phosphate, pH 7.0), whereas a unimolecular fold is dominant in a buffer which mimics the blood salt composition (137 mM NaCl, 2.7 mM KCl, 10 mM Na-phosphate, pH 7.4).[8] In comparison, our NMR data established the formation of a unimolecular fold of TBA at a wide concentration range of K^+ ions (10–110 mM KCl) under non-buffered conditions. Recently, CD and electrophoretic mobilities were used to establish bimolecular G-quadruplex formation of TBA at 110 mM K^+ (pH 6.1),[22] which is in contrast to the present and earlier[12] NMR studies at the same salt concentration and pH which clearly established the unimolecular fold.

The use of 2D NMR experiments enabled us to confirm that both topology and loop conformations are similar in the presence of $^{15}NH_4^+$ and K^+ ions. Furthermore, ^{15}N–^1H HSQC spectra complemented with ROESY experiments have shown unequivocally that $^{15}NH_4^+$ ions are localized between the two G-quartets in the interior of intramolecular G-quadruplex. Our NMR data give no indication of any other $^{15}NH_4^+$ ion binding site that is long-lived on the NMR time-scale. The equilibrium constant of $^{15}NH_4^+$ ion binding to a TBA G-quadruplex is 190 ± 30 M^{-1} at 15 °C. Similarity of ionic radii of $^{15}NH_4^+$ and K^+ ions suggests that K^+ ions bind between the two G-quartets of TBA G-quadruplex, which is also in accordance with the localization and coordination of Sr^{2+} and Pb^{2+} ions to the eight surrounding guanine C6-carbonyl groups.[15,17,18]

It is interesting to note that the bound $^{15}NH_4^+$ ions in ROESY spectra exhibited *ca.* 20% weaker cross-peaks with imino protons of G2 and G11 than with the other six guanines involved in the two G-quartets. This observation is interpreted in terms of out of plane bending of G2 and G11 towards the two TT loops away from the bound $^{15}NH_4^+$ ions. Such orientation of G2 and G11 residues out of the G-quadruplex core differs from the TBA structures established earlier in the presence of K^+ ions (PDB ID 148),[12] which showed out of plane bending of G2 towards the interior of the G-quadruplex, and Sr^{2+} ions (PDB ID 1RDE)[15] with almost perfect planarity of the G-quartets.

Exchange of $^{15}NH_4^+$ ions between the inner binding site and bulk solution is characterized by the exchange rate constant k_{1B} of 1.0 s^{-1} at 15 °C. Although it was not possible to experimentally verify through NzExHSQC spectra the exit/entry direction of $^{15}NH_4^+$ ions from/into the interior of the G-quadruplex core, the exchange cross-peaks between bulk $^{15}NH_4^+$ ions and residues of TGT loop in ROESY spectra suggested that movement of $^{15}NH_4^+$ ions proceeds preferentially through the G-quartet that is spanned by a T7–G8–T9 loop. The movement of $^{15}NH_4^+$ ions through the G-quartet on the opposite site of the G-quadruplex core is restricted by a noncannonical T4–T13 base pair. The exchange rate constant k_{1B} for TBA is in good agreement with the recently reported rate constant of 0.8 s^{-1} for $^{15}NH_4^+$ ion movement from the outer binding site of d[$(G_4T_3G_4)_2$] into bulk solution at 35 °C.[32] The slow movement of $^{15}NH_4^+$ ions from the outer binding site of the bimolecular d[$(G_4T_3G_4)_2$] quadruplex into bulk solution has been attributed to the steric hindrance imposed by the T_3 loops. Individual thymines are stacked over the outer G-quartets in d[$(G_4T_3G_4)_2$] and thus close the exit/entry of $^{15}NH_4^+$ ions into the central cation cavity. In comparison, T4 and T13 in the TBA G-quadruplex form a base pair and in this way add to the stiffness and stability of the TBA G-quadruplex, which also affects the rate of $^{15}NH_4^+$ ion movement through the outer G-quartet spanned by the two TT loops. The k_{1B} rate constant in the TBA quadruplex can also be compared to the exchange rate constant of 0.75 s^{-1} at 20 °C for the movement of $^{15}NH_4^+$ ions from the outer binding site to the bulk solution past the two T_4 lateral loops of unimolecular d[$G_4(T_4G_4)_3$] quadruplex.[30] Unfortunately, the comparison of exchange rate constants cannot be made at the same temperature due to specific melting temperature of each quadruplex as well as kinetics of cation movement, which can be too slow to detect at low temperatures. Nevertheless, the data suggest that the topology of loops is an important factor in controlling the rates of cation movement, but is not the sole determining factor.

Evaluation of ROESY spectra shows that volumes of cross-peaks between bulk water and imino protons of G2 and G11 are larger than with the other six guanines in G-quartets. This observation is in complete agreement with ROE interactions between bound $^{15}NH_4^+$ ions and the eight guanine imino protons, which affirmed that G2 and G11 exhibit out of plane bending towards the loop residues. Interestingly, imino protons of G2 and G11 were, in addition to G15, found to exchange faster than the other guanines in the presence of Sr^{2+} ions.[16] It is noteworthy that ROE cross-peaks of bulk water with G2 and G11 are larger than with the other six imino protons of guanines in G-quartets at low K^+ ion concentration. ROESY spectra, in addition, showed exchange cross-peaks between bulk $^{15}NH_4^+$ ions and imino protons of T3, T4, G8, T9, T12 and T13 suggesting cation interactions with thymine residues that are, however, short-lived. Analysis of exchange cross-peaks in ROESY spectra clearly shows a very close correspondence between the rigidity of individual structural elements and the chemical exchange of $^{15}NH_4^+$ ions and bulk water.

The equilibrium constant of $^{15}NH_4^+$ ion binding to TBA at 15 °C is 190 M^{-1}, which is considerably smaller than binding affinities of K^+ and Pb^{2+} ions with values around 10^7 M^{-1}.[17,35] This huge variation might originate from the nature of different experimental techniques, in addition to the intrinsic difference in binding constants of various cations. The equilibrium binding constant of Na^+ ions to TBA has been found to be around 10^5 M^{-1},[35] which is significantly higher in comparison to the $^{15}NH_4^+$ ion binding studied here. However, the above binding constants should be compared with care as our NMR data showed the presence of several different folds in the presence of Na^+ ions.

A survey of present and previously reported results demonstrates that TBA G-quadruplex formation, stability and structural characteristics are highly sensitive to the presence of specific cation and solution conditions. In this context, it is noteworthy that our study provides new structural details and complements them with flexibility of both G-quartets and loops as constituents of unimolecular TBA G-quadruplex, which has previously been shown to be a predominant form in conditions mimicking physiological environment in blood. Folding in the presence of $^{15}NH_4^+$ ions proved to be useful not only for determining the number, but also the location of cation binding site between the two G-quartets in the core of unimolecular TBA quadruplex, and not between the T7–G8–T9 loop and the neighbouring G-quartet and between the T3–T4 and T12–T13 loops and the G-quartet. In addition, interactions of $^{15}NH_4^+$ ions and water molecules in bulk solution with the nearby imino protons of TBA quadruplex

observed in ROESY spectra give a clear indication of out-of-plane bending of G2 and G11. Information on exposure of these two residues to the bulk solution is in agreement and complements proximity information between the bound $^{15}NH_4^+$ ions and imino protons of eight guanine residues involved in two G-quartets in the interior of TBA quadruplex. The topology of the TBA quadruplex with two TT loops on the same side of a G-quadruplex core, and a single lateral TGT loop on the opposite side of the structure also influences the dynamics of $^{15}NH_4^+$ ion movement from the interior of the chair-type G-quadruplex. The study of movement of $^{15}NH_4^+$ ions in a chair-type topology offers new insights on the role of lateral-type loops in controlling the passage of cations thought the central ion channel which have not been studied before. The results complement our previous data on $^{15}NH_4^+$ ion movement in G-quadruplexes of different topologies.[29,30,32] NMR data that provide experimental insights into both localization and cation movement are rather unique in structural studies of DNA in solution. G-Quadruplexes, with their tight binding of cations, represent a unique system that allows the study of the kinetics of cation movement in an aqueous solution.

Experimental

Oligonucleotides were synthesized on an Expedite 8909 synthesizer using standard phosphoramidite chemistry, deprotected with the use of aqueous ammonia, desalted and purified on a Sephadex G-15 column followed by extensive dialysis (Spectrapor) against LiCl solution. Oligonucleotide concentrations were between 1.5 and 2.6 mM. $^{15}NH_4Cl$, KCl and NaCl solutions were titrated into samples with the final aliquots not exceeding more than 5% of the sample volume. LiOH and HCl solutions were used to regulate the pH of the samples.

NMR data were collected on a Varian NMR System 600 and 800 MHz NMR spectrometers in the 0–25 °C temperature range. Standard 1D ^1H spectra in 95% ^1H_2O–5% ^2H_2O were acquired with the use of WATERGATE and DPFGSE solvent suppression methods. NOESY and ROESY spectra were acquired with mixing times between 40 and 250 ms. Intranucleotide connectivities between imino and aromatic protons were acquired on a natural abundance sample with the use of jump-and-return HMBC experiment. Thirty different gradient strengths (0.49-29.06 G cm^{-1}) were used in diffusion experiments. ^{15}N–^1H HSQC and a series of ^{15}N–^1H NzExHSQC spectra with mixing times in the range from 13 ms to 8 s were acquired at 15 °C. Cross-peaks were integrated with VNMRJ 2.1A software with the same chemical shift windows for all cross-peaks. Volumes of autocorrelation (V_{auto}) and cross-peaks (V_{cross}) in NzExHSQC spectra as a function of mixing time were interpreted by eqn (1) and 2, respectively:

$$V_{auto}(\tau_m) = A_1\left[e^{-B_1*\tau_m}\right] + A_2\left[e^{-B_2*\tau_m}\right] \quad (1)$$

where A_1 and A_2 are the scaling factors, B_1 and B_2 are rate constants and τ_m is the mixing time.

$$V_{cross}(\tau_m) = Af\left[e^{-\tau_m/T_1}\left(1-e^{-k_{IB}\tau_m}\right)\right] \quad (2)$$

where A is a scaling factor and is equal to the sum of A_1 and A_2 obtained through the analysis of the autocorrelation peak **I** by using eqn (1), parameter f defines the reduction of V_{cross} due to proton exchange, τ_m is the mixing time, k_{IB} is the exchange rate constant and T_1 is spin–lattice relaxation time.

Least-square fitting was done using Origin 7.5 software. Quality of the fits was monitored through parameter χ^2.

CD experiments were carried out on Applied Photophysics Chirascan CD spectrometer at 10.5 °C over the wavelength range 220–320 nm. Measurements were made in 0.1 cm path-length quartz cells. The oligonucleotide concentration was 50 μM and salt concentration was 100 mM.

Temperature-dependent melting curves were measured on a Perkin-Elmer Lambda Bio 40 spectrometer equipped with a Peltier temperature control system. A temperature range from 5 to 90 °C was used to monitor absorbance at 295 nm with 0.1 °C min^{-1} (melting/annealing rate). Measurements were made in 1 cm path-length cells.

Acknowledgements

We thank the Slovenian Research Agency (ARRS) and the Ministry of Higher Education, Science and Technology of the Republic of Slovenia (Grant Nos. P1-0242 and J1-0986) and COST Action MP0802 for their financial support. We are grateful to Professor Jean Louis Mergny for helpful discussions and to Igor Drobnak for help with UV measurement.

References

1 L. C. Bock, L. C. Griffin, J. A. Latham, E. H. Vermaas and J. J. Toole, *Nature*, 1992, **355**, 564.
2 I. Smirnov and R. H. Shafer, *Biochemistry*, 2000, **39**, 1462.
3 C. F. Tang and R. H. Shafer, *J. Am. Chem. Soc.*, 2006, **128**, 5966.
4 L. Martino, A. Virno, A. Randazzo, A. Virgilio, V. Esposito, C. Giancola, M. Bucci, G. Cirino and L. Mayol, *Nucleic Acids Res.*, 2006, **34**, 6653.
5 A. Virno, A. Randazzo, C. Giancola, M. Bucci, G. Cirinoc and L. Mayol, *Bioorg. Med. Chem.*, 2007, **15**, 5710.
6 B. Pagano, L. Martino, A. Randazzo and C. Giancola, *Biophys. J.*, 2008, **94**, 562.
7 G. Mayer, J. Müller, T. Mack, D. F. Freitag, T. Höver, B. Pötzsch and A. Heckel, *ChemBioChem*, 2009, **10**, 654.
8 T. Coppola, M. Varra, G. Oliviero, A. Galeone, G. D'Isa, L. Mayol, E. Morelli, M. R. Bucci, V. Vellecco, G. Cirino and N. Borbone, *Bioorg. Med. Chem.*, 2008, **16**, 8244.
9 R. F. Macaya, P. Schultze, F. W. Smith, J. A. Roe and J. Feigon, *Proc. Natl. Acad. Sci. U. S. A.*, 1993, **90**, 3745.
10 K. Y. Wang, S. N. McCurdy, R. G. Shea, S. Swaminathan and P. H. Bolton, *Biochemistry*, 1993, **32**, 1899.
11 K. Y. Wang, S. H. Krawczyk, N. Bischofberger, S. Swaminathan and P. H. Bolton, *Biochemistry*, 1993, **32**, 11285.
12 P. Schultze, R. F. Macaya and J. Feigon, *J. Mol. Biol.*, 1994, **235**, 1532.
13 J. A. Kelly, J. Feigon and T. O. Yeates, *J. Mol. Biol.*, 1996, **256**, 417.
14 B. I. Kankia and L. A. Marky, *J. Am. Chem. Soc.*, 2001, **123**, 10799.
15 X. A. Mao, L. A. Marky and W. H. Gmeiner, *J. Biomol. Struct. Dyn.*, 2004, **22**, 25.
16 X. Mao and W. H. Gmeiner, *Biophys. Chem.*, 2005, **113**, 155.
17 I. Smirnov and R. H. Shafer, *J. Mol. Biol.*, 2000, **296**, 1.
18 I. V. Smirnov, F. W. Kotch, I. J. Pickering, J. T. Davis and R. H. Shafer, *Biochemistry*, 2002, **41**, 12133.
19 M. Vairamani and M. L. Gross, *J. Am. Chem. Soc.*, 2003, **125**, 42.
20 K. Y. Wang, S. Kumar, T. Q. Pham, V. M. Marathias, S. Swaminathan and P. H. Bolton, *J. Mol. Biol.*, 1996, **260**, 378.
21 I. V. Smirnov and R. H. Shafer, *Biopolymers*, 2007, **85**, 91.
22 M. Fialova, J. Kypr and M. Vorlickova, *Biochem. Biophys. Res. Commun.*, 2006, **344**, 50.
23 V. M. Marathias and P. H. Bolton, *Biochemistry*, 1999, **38**, 4355.
24 V. M. Marathias and P. H. Bolton, *Nucleic Acids Res.*, 2000, **28**, 1969.
25 N. V. Hud, P. Schultze and J. Feigon, *J. Am. Chem. Soc.*, 1998, **120**, 6403.

26 N. V. Hud, P. Schultze, V. Sklenar and J. Feigon, *J. Mol. Biol.*, 1999, **285**, 233.
27 P. Sket, M. Crnugelj, W. Kozminski and J. Plavec, *Org. Biomol. Chem.*, 2004, **2**, 1970.
28 P. Sket, M. Crnugelj and J. Plavec, *Nucleic Acids Res.*, 2005, **33**, 3691.
29 P. Sket and J. Plavec, *J. Am. Chem. Soc.*, 2007, **129**, 8794.
30 P. Podbevsek, N. V. Hud and J. Plavec, *Nucleic Acids Res.*, 2007, **35**, 2554.
31 P. Podbevsek, P. Sket and J. Plavec, *Nucleosides, Nucleotides Nucleic Acids*, 2007, **26**, 1547.
32 P. Podbevsek, P. Sket and J. Plavec, *J. Am. Chem. Soc.*, 2008, **130**, 14287.
33 B. I. Kankia, G. Barany and K. Musier-Forsyth, *Nucleic Acids Res.*, 2005, **33**, 4395.
34 S. Nagatoishi, Y. Tanaka and K. Tsumoto, *Biochem. Biophys. Res. Commun.*, 2007, **352**, 812.
35 N. Kumar and S. Maiti, *Biochem. Biophys. Res. Commun.*, 2004, **319**, 759.
36 M. Cevec and J. Plavec, *Biochemistry*, 2005, **44**, 15238.
37 M. X. Fernandes, A. Ortega, M. C. L. Martinez and J. G. de la Torre, *Nucleic Acids Res.*, 2002, **30**, 1782.

